Journal of Alloys and Compounds 509 (2011) 6317–6320

Contents lists available at ScienceDirect

Journal of Alloys and Compounds

journal homepage: www.elsevier.com/locate/jallcom

Low-voltage cathodoluminescence properties of green-emitting $ZnAl_2O_4:Mn^{2+}$ nanophosphors for field emission display

Xiaojun Wang, Mingchang Zhang, Hui Ding, Huili Li*, Zhuo Sun

Engineering Research Center for Nanophotonics and Advanced Instrument, Ministry of Education, Department of Physics, East China Normal University, No. 3663 North Zhongshan Rd., Shanghai 200062, China

ARTICLE INFO

Article history:
Received 21 December 2010
Received in revised form 10 March 2011
Accepted 10 March 2011
Available online 21 March 2011

Keywords:
$ZnAl_2O_4:Mn^{2+}$
Coprecipitation method
Phosphors
Cathodoluminescence
FED

ABSTRACT

A low-cost $ZnAl_2O_4:Mn^{2+}$ green nanophosphor for field emission display (FED) was successfully synthesized by the coprecipitation method and a two-step firing, firstly calcining at 1200 °C for 2 h in air and then annealing at 900 °C for 3 h in flowing NH_3 gas. The effects of the preparation process and the Mn^{2+} concentration on optical properties of $ZnAl_2O_4:Mn^{2+}$ were investigated. The phase composition, particle morphology, photoluminescence (PL) spectra of the $ZnAl_2O_4:Mn^{2+}$ phosphor as well as low-voltage field emission properties of the FED device prepared by using the synthesized $ZnAl_2O_4:Mn^{2+}$ phosphor were examined. Similar to $ZnGa_2O_4:Mn^{2+}$, Mn^{2+}-doped $ZnAl_2O_4$ showed two green emission bands centered at 508 and 517 nm, respectively, which originate from $^4T_1(^4G)\rightarrow{}^6A_1(^6S)$ transitions of Mn^{2+} on T_d and O_h sites. The PL intensity reached the maximum at 0.5 at.% Mn^{2+}. Under the low-voltage excitation, the FED device exhibited bright green emission, high voltage brightness saturation, and high color purity.

1. Introduction

Recently, field emission display (FED) has been studied extensively as the next-generation full color flat panel display device. In comparison to the conventional cathode-ray tubes (CRT), FED technology requires a phosphor screen to be operated under a lower electron accelerating voltage, typically 1–5 kV. Therefore, phosphors for FED should possess the features of: (i) high efficiency under the low-voltage excitation; (ii) high resistance to current saturation, high chemical and thermal stability, and long lifetime at high current density; (iii) good thermal and electrical conductivity [1,2].

It is well-known that manganese-doped $ZnGa_2O_4$ spinel ($ZnGa_2O_4:Mn^{2+}$) exhibits green emission corresponding to the d-d transition of Mn^{2+} under the UV light or electron beam excitation, as well as high chemical stability in comparison to other phosphors such as sulfides and oxysulfides. Therefore, it has been successfully used in flat-panel displays as a low-voltage oxide phosphor [3–7]. However, the high cost of source materials containing Ga limits its application to optical devices. As an alternative, $ZnA1_2O_4:Mn^{2+}$ could be an interesting FED phosphor because Al and Ga belong to the same IIIA family in the periodic table. Most importantly, starting materials containing Al are much cheaper and easier to be acquired.

Similar to $ZnGa_2O_4$, zinc aluminate ($ZnA1_2O_4$) is also a well-known wide-band gap semiconductor which has an optical bandgap of about 3.8 eV [8,9]. It has attracted many interests as a phosphor host material for applications to thin film electroluminescent displays, mechano-optical stress sensors, and stress imaging devices because of its moderate conductivity, high thermal and chemical stability, and good optical and catalytic properties. Green electroluminescence (EL) and stress-stimulated luminescence have been observed in the Mn-doped $ZnA1_2O_4$ film and powder [10–14]. Recently, nanostructured $ZnA1_2O_4:Mn^{2+}$ phosphors have been studied intensively and successfully prepared by a simple sol–gel and combustion method. Under the electron beam irradiation in vacuum, intense cathodoluminescence (CL) with high chromaticity was observed. The CL intensity can be enhanced by the careful control of the cationic molar ratio of Zn to Al atoms and a post-synthesis treatment [9,13,15,16]. The above results suggest that Mn-doped $ZnAl_2O_4$ would be a good green-emitting CL phosphor for low-voltage FEDs. However, up to now, there is no report on its application to FED device.

In this work, Mn-doped $ZnAl_2O_4$ nanophosphors will be prepared by the coprecipitation method. The phase evolution, microstructure, and photoluminescence (PL) properties of synthesized powders are characterized by X-ray diffraction (XRD), filed-emission scanning electron microscopy (FESEM), and fluorescence spectrophotometer, respectively. The influence of the dopant concentration on optical properties is also investigated. Finally, the phosphor screens as an anode plate with a size of 1 cm × 1 cm are

* Corresponding author. Tel.: +86 21 62235465; fax: +86 21 62234321.
E-mail address: hlli@phy.ecnu.edu.cn (H. Li).

0925-8388/$ – see front matter © 2011 Elsevier B.V. All rights reserved.
doi:10.1016/j.jallcom.2011.03.076

prepared by using the synthesized $ZnAl_2O_4:Mn^{2+}$ and their low-voltage CL characteristics will be discussed in details.

2. Experimental

$Zn_{1-x}Mn_xAl_2O_4$ nanophosphors with $x = 0.003–0.020$ were synthesized by the coprecipitation method. Zinc nitrate hexahydrate ($Zn(NO_3)_2·6H_2O$, >99.0%, analytical grade, Sinopharm Chemical Reagent Co., Ltd.), aluminium nitrate nonahydrate ($Al(NO_3)_3·9H_2O$, >99.0%, analytical grade, Sinopharm Chemical Reagent Co., Ltd.) and manganese(II) acetate tetrahydrate($C_4H_6MnO_4·4H_2O$, >99.0%, analytical grade, Sinopharm Chemical Reagent Co., Ltd.) were used as starting materials in the present work. Ammonium bicarbonate (NH_4HCO_3, >99.0%, analytical grade, Sinopharm Chemical Reagent Co., Ltd.) was used as a precipitant.

Stoichiometric amount of $Zn(NO_3)_2·6H_2O$, $Al(NO_3)_3·9H_2O$ and $C_4H_6MnO_4·4H_2O$ were firstly dissolved in deionized water according to the target compositions of $Zn_{1-x}Mn_xAl_2O_4$ ($x = 0.003–0.020$) to form the transparent stock solution of mother salts. The concentration of Zn^{2+} was 0.01 M. 2 M ammonium bicarbonate solution was then prepared and used as the precipitant solution. The precursor precipitate was produced by adding the mixed salt solution at a speed of 3 ml/min from a burette into the ammonium bicarbonate solution under the mild agitation at room temperature (RT). During the coprecipitation, a pH value of 8 was kept constant. For multi-cations materials, the reverse strike technique has the advantage of higher cation homogeneity in the precursor. The slurry obtained was aged for 12 h with agitation by a magnetic agitator. Subsequently, the precipitation was filtered and washed repeatedly with deionized water and alcohol to completely remove the by-products of the reaction. After that, the resulting product was dried at 80 °C for 12 h. The dried cake was crushed with an agate pestle and mortar. Finally, the precursor powder was placed in an alumina crucible and calcined at 800–1200 °C for 2 h in an alumina tubular furnace in air. This finally leads to $ZnAl_2O_4$ crystallines and oxidizes a little amount of remanent CH_3COO^- group. Simultaneously, Mn^{2+} in the starting materials may be oxidized to higher valences such as Mn^{3+} and Mn^{4+}, which will affect the luminescent properties of phosphors. Therefore, the as-synthesized phosphors were then post heat-treated at 900 °C for 3 h in flowing NH_3 gas atmosphere.

X-ray powder diffraction (XRD) patterns of the precursor and calcined powders were recorded on a D8 ADVANCE X-ray diffractometer with the Cu Kα radiation at 40 kV and 40 mA. The morphology of $ZnAl_2O_4:Mn^{2+}$ phosphor was observed by a field-emission scanning electron microscope (FESEM, Hitachi S4700). PL spectra at RT were examined by a fluorescence spectrophotometer (Horiba Jobin Yvon, FluoroMax-4). The low-voltage field emission properties of phosphor screens were measured by a chroma meter (CS-100A) in a vacuum chamber with the base pressure of 10^{-5} Pa at RT. The anode of phosphor screens coated on an indium tin oxide (ITO) glass plate by the screen printing was separated from the carbon nanotubes (CNTs) film cathode by a teflon foil with a thickness of 270 μm. A simple FED device with a parallel diode-type configuration was assembled by the phosphor screen anode and the CNTs film cathode, as seen in Fig. 1 [17]. The measured emission area was fixed at 1 cm × 1 cm.

3. Results and discussion

Fig. 2 shows XRD patterns of the as-prepared $ZnAl_2O_4$:0.5 at.% Mn precursor and powders calcined at various temperatures for 2 h. It can be noted that the resultant precursor after drying is almost amorphous, and no obvious diffraction peaks are identified. After calcined at 800 °C in air, all the characteristic peaks of the cubic $ZnAl_2O_4$ spinel phase appear, which indicates that the $ZnAl_2O_4$ cubic phase starts to crystallize at this temperature.

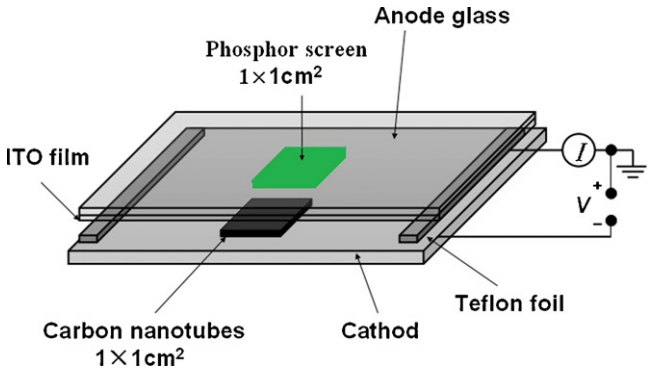

Fig. 1. Parallel diode-type configuration sketch for field-emission testing.

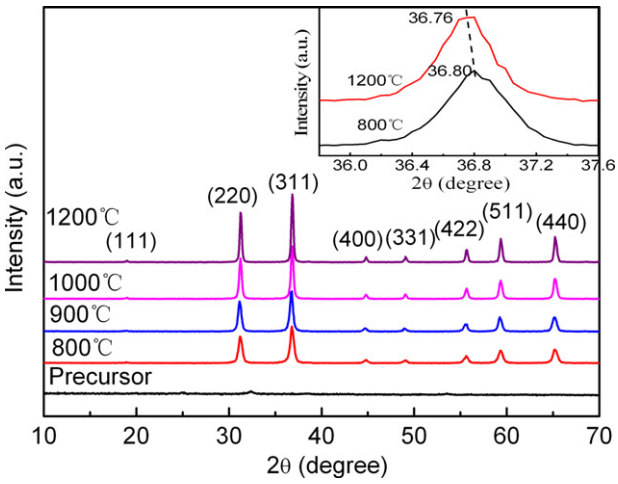

Fig. 2. XRD patterns of the precursor and powder of $ZnAl_2O_4$:0.5 at.% Mn calcined at various temperatures for 2 h; The inset shows the XRD peak in (3 1 1) plane.

As the annealing temperature increases from 800 to 1200 °C, the diffraction peaks sharpen and the intensity continuously increases, suggesting that the $ZnAl_2O_4$ crystallites gradually grow. Moreover, the diffraction patterns shift to the lower angel as seen in the inset of Fig. 2. The difference of $\Delta\theta = 0.04°$ between the peak position of the sample annealed at 800 °C and that of the sample annealed at 1200 °C indicates that the lattice constant is slightly increased due to the partial replacement of the smaller Zn^{2+} (74 pm) by the larger Mn^{2+} (80 pm) [5,18]. In addition, the removal of oxygen vacancies in the lattice or surface defects due to the high temperature oxidation can also contribute to such a lattice expansion as well as better crystallinity [19,20]. Generally, the better crystallinity of a phosphor can obviously improve the optical properties, such as luminescecnt intensity, quantum efficiency, and thermal stability. Therefore, in the following experiments, the calcining temperature of the first step is fixed at 1200 °C.

Fig. 3 shows the FESEM micrograph of the Mn-doped $ZnAl_2O_4$ phosphor calcined at 1200 °C for 2 h in air. It can be seen that the phosphor prepared by the coprecipitation method shows relatively uniform, dispersive, and nearly spherical morphology. The average particle size is about 50 nm. It is well known that the luminescent properties of a phosphor powder are dependent upon its particle size and size distribution. Finer particles tend to have more surface luminous states arising from their increased surface/bulk

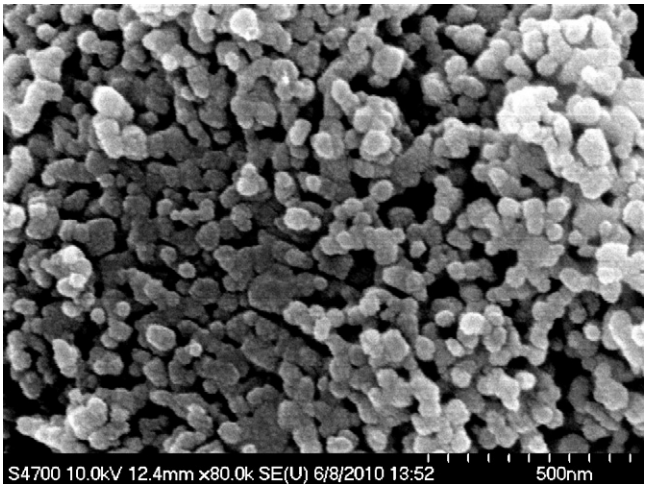

Fig. 3. FESEM image of the $ZnAl_2O_4$:0.5 at.% Mn phosphor calcined at 1200 °C for 2 h.

volume ratio. This may result in different luminescent properties from the bigger ones [21,22]. Phosphor particles with a uniform size are thus beneficial to highly efficient and uniform luminescence [23]. For the practical application of $ZnAl_2O_4$:Mn^{2+} phosphors to FED, smaller particle size, narrower size distribution, and nearly spherical shape would improve the resolution of the display device by decreasing the pixel size. Simultaneously, a denser and uniform phosphor layer would be formed on the substrate through the close packing of phosphor spheres, which can prolong the lifetime of the device and improve its stability. Therefore, by using such kind of phosphors, the luminescent efficiency and the brightness of the phosphor panel are expected to be improved. In addition, a small amount of aggregates can be also observed because of the high sintering temperature.

The excitation and emission spectra of $ZnAl_2O_4$ doped with 0.5 at.% Mn fired at different conditions are present in Fig. 4. Obviously, the firing process has a great influence on PL properties of the synthesized $ZnAl_2O_4$:Mn. The sample annealed at 1200 °C for 2 h in air shows only a weak blue–green emission band centered at 490 nm and a broad weak excitation band ranging from 306 to 400 nm. The body color of the phosphor is brown, which could be attributed to the oxidation of most Mn^{2+} to higher valence (Mn^{3+} and Mn^{4+}) in air. When the sample was only fired at 1200 °C for 3 h in a gas flow of NH_3, the PL spectrum is similar to that of the sample calcined in air, showing a relatively lower intensity. In a strong NH_3 reducing atmosphere, a small amount of remanent CH_3COO^- group cannot be completely oxidized, which leads to the residual carbon. Therefore, the calcined phosphors are black, which have very low luminescence. However, when powders were firstly fired in air and then reduced in flowing NH_3, the intense green emission from Mn^{2+} is detected. The corresponding daylight color changes from brown to white due to the reduction of manganese ions from the higher valences to Mn^{2+}. Under the excitation of 310 nm, the emission spectrum consists of two bands resulting from $^4T_1$ (^4G)→$^6A_1$ (^6S) transitions of Mn^{2+} [24,25]. One peak locates at 508 nm and the other one at 517 nm. Two emission bands are attributed to two different sites of Mn^{2+} ions: tetrahedrally coordinated Zn^{2+} sites surrounded by four oxygens [$Mn^{2+}_{Zn^{2+}}$ (T_d)] and octahedrally coordinated Al^{3+} sites surrounded by six oxygens [$Mn^{2+}_{Al^{3+}}$ (O_h)], respectively. It is known that the emission of Mn^{2+} strictly depends on its coordination number in the host material and the size of the crystallographic site where it occupies [26,27]. Two different Mn^{2+} ions experience the different crystal field strength as a result of the different environment. The crystal field of Mn^{2+} ions at O_h sites

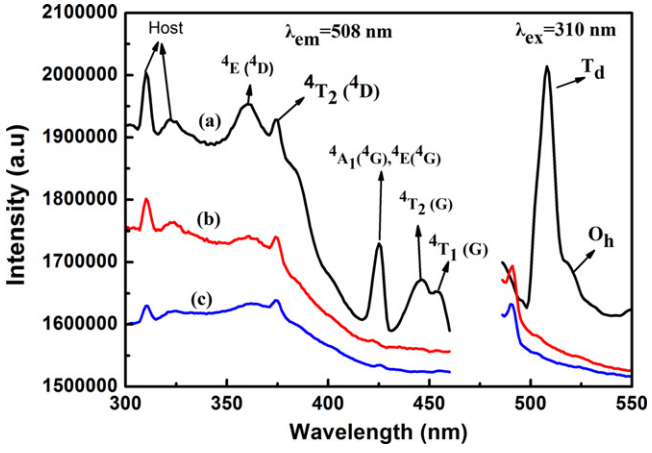

Fig. 4. Excitation and emission spectra of the $ZnAl_2O_4$:0.5 at.% Mn phosphors fired in different atmosphere: (a) 1200 °C for 2 h in air and post heat-treated at 900 °C for 3 h in NH_3; (b) 1200 °C for 2 h in air; and (c) 1200 °C for 2 h in NH_3.

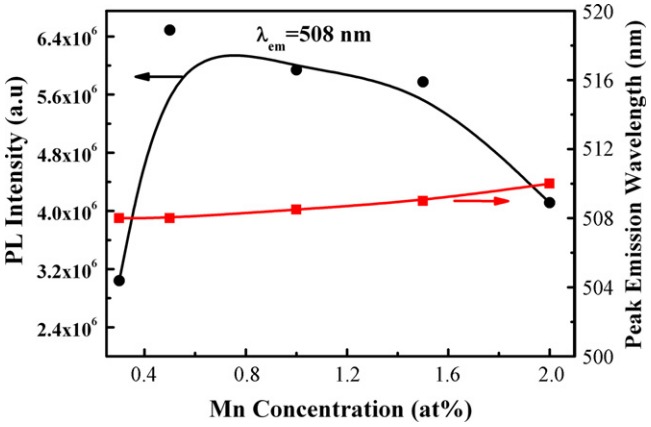

Fig. 5. The PL intensity and peak emission wavelength at 508 nm as a function of Mn^{2+} concentration.

is stronger because they are coordinated to more neighboring ions, which leads to the red shift of the emission wavelength [28]. Therefore, the peak at 517 nm can be assigned to Mn^{2+} on O_h sites, and the peak at 508 nm can be attributed to Mn^{2+} on T_d sites. These results are consistent with PL spectra of Mn^{2+}-doped $ZnGa_2O_4$ reported by Kim et al. [5]. It is confirmed that $ZnAl_2O_4$:Mn^{2+} powder is also a good green-emitting phosphor. The broad excitation band in the wavelength range of 306–460 nm can be observed with the monitoring wavelength of 508 nm. Definitely, the strong excitation bands below 330 nm originate from the host lattice absorption, as can be concluded from the wide band gap of 3.8 eV of $ZnAl_2O_4$ [7,8]. The appearance of the host lattice absorption bands in the excitation spectrum indicates that there exists an efficient energy transfer from the host lattice to Mn^{2+} ions. The remaining excitation bands in the wavelength range of 330–460 nm can be assigned to the transitions of Mn^{2+} from ground state $^6A_1$ (^6S) to ^4E (^4D), $^4T_2$ (4D), [$^4A_1$(^4G), ^4E(^4G)], $^4T_2$ (^4G) and $^4T_1$ (^4G) levels, respectively. Excitingly, the obvious excitation peaks at 446 and 455 nm could make $ZnAl_2O_4$:Mn^{2+} to be a suitable green phosphor for white LEDs using blue LED chips.

Fig. 5 shows the dependence of PL intensity and the peak emission wavelength at 508 nm of the $ZnAl_2O_4$:Mn^{2+} phosphors with varying Mn^{2+} concentrations. It can be seen that the PL intensity at 508 nm (T_d) rapidly increases with the Mn^{2+} content increasing from 0.3 to 0.5 at.% and reaches the maximum at about 0.5 at.%. Above this concentration, the concentration quenching occurs. Meanwhile, no obvious shift in the peak emission wavelength is observed with the Mn^{2+} concentration varying from 0.3 to 2.0 at.%. It may be attributed to the low doping concentration and no overlap between the excitation and emission spectrum. The above phenomenon can also be observed for the emission band at 517 nm (O_h), but, the emission intensity ratio of Mn^{2+} ions at 508 nm to that at 517 nm keeps unchanged when the Mn^{2+} concentrations increase, suggesting that the ratio of Mn^{2+} ions on T_d sites to O_h sites does not vary with its concentration.

In order to investigate the low-voltage field emission properties of phosphors synthesized in the present work, a simple FED device with a parallel diode-type configuration was prepared, as seen in Fig. 1. It consists of two parts: the phosphor screen anode and the CNTs film cathode. The measured area is fixed at 1 cm × 1 cm. Fig. 6 shows the luminous efficiency of the FED device prepared by using the synthesized $ZnAl_2O_4$:0.5 at.% Mn^{2+} phosphor excited by different voltages. As expected, the luminous efficiency remarkably enhances with an increase in the accelerating voltage. Moreover, no brightness saturation occurs even at 700 V, which is very useful for highly efficient FED devices. The

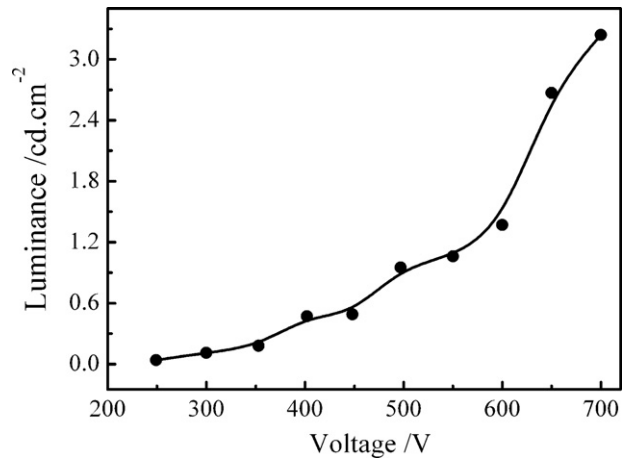

Fig. 6. Dependence of luminous efficiency of the $Zn_{0.995}Mn_{0.005}Al_2O_4$ phosphor screen with 1 cm × 1 cm on the excitation voltage.

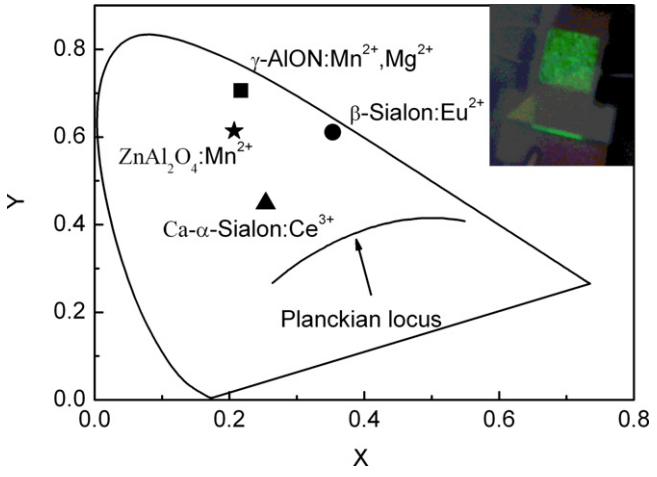

Fig. 7. Chromaticity coordinates of Mn^{2+}-doped $ZnAl_2O_4$. The inset shows a photograph of FED flat device by using $ZnAl_2O_4$:Mn^{2+} on excitation at 500 V. The blackbody radiation locus is indicated by the solid curve.

increase in luminous efficiency with an increase of acceleration voltage is attributed to the deeper penetration of electrons into the phosphor body, the larger electron beam current density, and the better electrical conductivity of $ZnAl_2O_4$. The chromaticity coordinates of $ZnAl_2O_4$ with 0.5 at.% Mn^{2+} are $x = 0.207$ and $y = 0.614$, as shown in Fig. 7. Compared to other green phosphors, such as β-Sialon:Eu^{2+} and γ-AlON:Mn^{2+},Mg^{2+}, $ZnAl_2O_4$:Mn^{2+} exhibits higher color purity, which enables to achieve a larger color gamut for devices. A photograph of an FED flat device by using $ZnAl_2O_4$:Mn^{2+} as the emission phosphor excited by 500 V is present in the insert of Fig. 7. The promising features of the phosphor, such as relatively uniform and dispersive morphology, small particle size, high voltage brightness saturation, and high color purity, make $ZnAl_2O_4$:Mn^{2+} a very attractive green phosphor for FED flat devices.

4. Conclusions

Uniform and dispersive $ZnAl_2O_4$:Mn^{2+} nanophosphors for FEDs were successfully prepared by the coprecipitation method. The influence of the Mn concentration on the photoluminescence was investigated. The phosphor firstly fired at 1200 °C for 2 h in air and then reduced at 900 °C for 3 h in flowing NH_3 show two green emission bands centered at 508 and 517 nm, which originate from Mn^{2+} ions on T_d and O_h sites. The concentration quenching occurs at 0.5 at.%. A simple FED device was prepared for the first time by using the synthesized $ZnAl_2O_4$:Mn^{2+} nanophosphor. Under the low-voltage excitation, it exhibits bright green emission, high voltage brightness saturation, and high color purity.

Acknowledgements

The authors greatly acknowledge financial supports from National Natural Science Foundation of China (No. 50902050), the Fundamental Research Funds for the Central Universities (No. 78210002), Shanghai Baiyulan Foundation (No. 2010B026), and Special Project for Solid-State Lighting Engineering and Optoelectronics of Shanghai (No. 09DZ1141900).

References

[1] Z.D. Lou, J.H. Hao, Thin Solid Films 450 (2004) 334–340.
[2] S. Shionoya, W.M. Yen, H. Yamamoto, Phosphor Handbook, second ed., CRC Press, Boca Raton, 2006.
[3] J.H. Park, B.W. Park, N.S. Choi, Y.T. Jeong, J.S. Kim, J.S. Yang, Electrochem. Solid State Lett. 11 (2008) J12–J14.
[4] W.J. Chang, H.L. Park, S.W. Mho, J.S. Park, J.C. Choi, G.C.J.H. Kim, Park, J.S. Kim, J. Korean Phys. Soc. 50 (2007) 1687–1691.
[5] J.S. Kim, T.W. Kim, S.M. Kim, H.L. Park, Appl. Phys. Lett. 86 (2005) 091912–91921.
[6] M. Takesada, T. Isobe, H. Takahashi, S. Itoh, J. Electrochem. Soc. 154 (4) (2007) J136–J140.
[7] M. Takesada, M. Osada, T. Isobe, J. Phys. Chem. Solids 70 (2009) 281–285.
[8] K. Kumar, K. Ramamoorthy, P.M. Koinkar, R. Chandramohan, K. Sankaranarayanan, J. Nanopart. Res. 9 (2007) 331–335.
[9] M.-T. Tsai, Y.-X. Chen, P.-J. Tsai, Y.-K. Wang, Thin Solid Films 518 (2010) e9–e11.
[10] H. Matsui, C.N. Xu, H. Tateyama, Appl. Phys. Lett. 78 (2001) 1068–1070.
[11] W. Staszaka, M. Zawadzki, J. Okala, J. Alloys Compd. 492 (2010) 500–507.
[12] C. Ma, X.Y. Chen, S.P. Bao, Micropor. Mesopor. Mater. 129 (2010) 37–41.
[13] Z. Lou, J. Hao, Appl. Phys. A: Mater. Sci. Process. 80 (2005) 151–154.
[14] W. Walerczyk, M. Zawadzki, J. Okal, Appl. Surf. Sci. 257 (2011) 2394–2400.
[15] T. Nagura, H. Kominami, Y. Nakanishi, K. Hara, Jpn. J. Appl. Phys. 48 (2009) 092302–092306.
[16] S.S. Pitale, V. Kumar, I.M. Nagpure, O.M. Ntwaeaborwa, H.C. Swart, Appl. Surf. Sci. 257 (2011) 3298–3306.
[17] M.C. Zhang, X.J Wang, H. Ding, H.L. Li, L.K. Pan, Z. Sun, Int. J. Appl. Ceram. Technol. doi:10.1111/j.1744-7402.2010.02542.x.
[18] M. Takesada, M. Osada, T. Isobe, J. Electrochem. Soc. 156 (5) (2009) J97–J101.
[19] J.S. Kim, H.I. Kang, W.N. Kim, J.I. Kim, J.C. Choi, H.L. Park, G.C. Kim, T.W. Kim, Y.H. Hwang, S.I. Mho, M.C. Jung, M. Han, Appl. Phys. Lett. 82 (2003) 2029–2031.
[20] S. Chakrabarti, D. Ganguli, S. Chaudhuri, J. Phys. D 36 (2003) 146–151.
[21] I. Yu, Mater. Res. Bull. 41 (2006) 1403–1406.
[22] S.H. Shin, J.H. kang, D.Y. Jeon, D.S. Zang, J. Solid State Chem. 178 (2005) 2205–2210.
[23] J.G. Li, X.D. Li, X.D. Sun, T. Ishigaki, J. Phys. Chem. C 112 (2008) 11707–11716.
[24] J.S. Kim, H.L. Park, G.C. Kim, T.W. Kim, Y.H. Hwang, H.K. Kim, S.I. Mho, S.D. Han, Solid State Commun. 126 (2003) 515–518.
[25] T.K. Tran, W. Park, J.W. Tomm, B.K. Wagner, S.M. Jacobsen, C.F. Summers, P.N. Yocom, S.K. McClelland, J. Appl. Phys. 78 (1995) 5691–5695.
[26] R.J. Xie, N. Hirosaki, X.J. Liu, T. Takeda, H.L. Li, Appl. Phys. Lett. 92 (2008) 201905–201911.
[27] C.J. Duan, W.M. Otten, A.C.A. Delsing, H.T. Hintzen, J. Solid State Chem. 181 (2008) 751–757.
[28] B. Henderson, G.G. Imbush, Optical Spectroscopy of Inorganic Solids, Clarendon, Oxford, 1989.